NMR Probing of Spin Excitations in the Ring Structure of a Two-Subband System

X. C. Zhang, G. D. Scott, and H. W. Jiang
Department of Physics and Astronomy, University of California at Los Angeles, 405 Hilgard Avenue, Los Angeles, California 90095, USA
(Received 30 October 2006; published 14 June 2007)

Resistively detected nuclear magnetic resonance (NMR) is observed inside the ringlike structure, with a quantized Hall conductance of $6e^2/h$, in the phase diagram of a two-subband electron system. The NMR signal persists up to 470 mK and is absent in other states with the same quantized Hall conductance. The nuclear spin-lattice relaxation time T_1, is found to decrease rapidly towards the ring center. A strong dynamic nuclear polarization by the biasing current has also been observed only inside the ring. These observations are consistent with the assertion of the ringlike region being a ferromagnetic state that is accompanied by collective spin excitations.

DOI: 10.1103/PhysRevLett.98.246802 PACS numbers: 73.43.Nq, 71.30.+h, 72.20.My

A two-dimensional electron system consisting of two filled subbands is emerging as an experimental laboratory to study charge and spin correlation effects. The correlations become particularly prominent when the two sets of Landau levels (LLs) with different subband quantum numbers are brought into degeneracy by varying magnetic field and/or carrier concentration. A series of experimental observations were made to explore the consequences of intrinsic electron spin exchange interactions [1,2], as well as pseudospin charge excitations in the vicinity of the degeneracy regions [3,4].

One of the interesting findings in the recent studies of the two-subband system is that the experimental phase diagram, in the density-magnetic field plane, exhibits pronounced ''ringlike structures'' at even integer filling factors [1]. It was conjectured that these structures represent ferromagnetic phases. This conjecture was based on theoretical predictions that a ferromagnetic phase transition can occur when two LLs with opposite spin are close to crossing at the Fermi energy. By promoting all the electrons, or holes, in the uppermost occupied LL to the lowest unoccupied LL of opposite spin, the total energy of the system can be lowered by the exchange mechanism [5]. Such a transition has been seen in a single subband two-dimensional hole system when two LLs with opposite spin and different LL index approach each other by increasing the Zeeman energy in tilted magnetic fields [6]. The ringlike structures have also been observed recently by Ellenberger *et al.* on a two-subband parabolic quantum well [2]. The authors, however, suggest that the ring structures can be single particle states with an enhanced exchange interaction within each subband in the framework of mean-field theory.

To address the question whether the ring structures are collective states in nature, measurements other than the conventional transport are needed. The resistively detected NMR technique has recently emerged as an effective method to probe collective spin states in the fractional quantum Hall regime [7,8], the Skyrmion spin texture close to the filling factor $\nu = 1$ [9,10], and the role of electron spin polarization in the phase transition of a bilayer system [11]. This method is significantly less demanding than the high-sensitivity conventional NMR detection [12]. Here we have adapted this technique to study NMR in the vicinity of the ring structure with a quantized Hall conductance of $6e^2/h$. It reveals that the NMR signal is phase-space dependent and only appears inside the ring structure. An array of observations suggests that the ringlike region is a collective state that has intriguing spin excitations.

The sample used in this study is a symmetrical modulation-doped single quantum well [13]. Both well and spacer are 240 Å thick. The total electron density at gate voltage $V_g = 0$ is 8.1×10^{11} cm^{-2}, with a distribution of 5.4 and 2.7×10^{11} cm^{-2} in the first and second subband, respectively. The mobility is 4.1×10^5 cm^2/V $\cdot$ s. A NiCr top gated 100 μm wide Hall bar with 270 μm between voltage probes was patterned by standard lithography techniques. Several turns of NMR coil were wound around the sample, which was placed in a dilution refrigerator with a base temperature of 60 mK, and in a perpendicular magnetic field normal to the sample plane. A small rf magnetic field generated by the coil with a matching frequency $f = \gamma H_0$ will cause NMR for ^{75}As nuclei, where the gyromagnetic ratio $\gamma = 7.29$ MHz/T. The resistance was measured using quasi-dc lock-in techniques with $f = 13.2$ Hz. The external magnetic field was calibrated within an accuracy of $\pm 0.1\%$, using the strong resistively detected NMR signal found at $\nu = 1.45$ and $B = 4.55$ T.

Figure 1 shows the phase diagram of longitudinal resistivity, ρ_{xx}, as a function of magnetic field, B, and carrier density, n, at 70 mK. Its most salient feature is the ringlike structure centered around the $\nu = 6$ line. It was previously speculated that the ring represents a ferromagnetic state, while on either side of the ring the system is in a paramagnetic state with exactly the same quantized Hall conductance, $6e^2/h$, because the topmost two occupied LLs are two spin split states of the same subband. The schematic

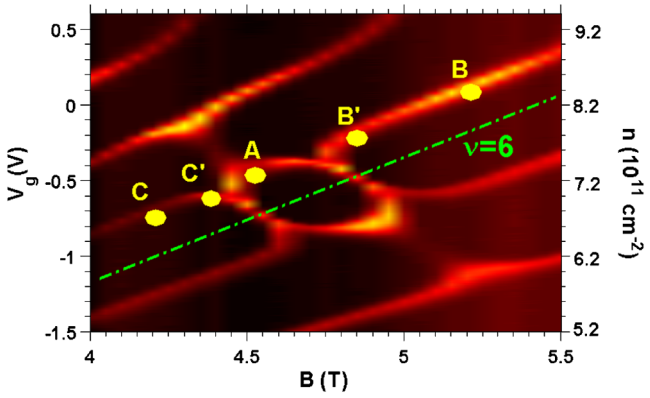

FIG. 1 (color online). Gray scale plot of resistivity versus magnetic field and gate voltage (or carrier concentration) at 75 mK. The filling factor $\nu = 6$ is shown by the dot-dashed line. Dots marked by A, B, B', C, and C' are the places where NMR experiments were conducted.

diagram for this model is illustrated in Fig. 5 of Ref. [1]. Recently the ringlike structures have been numerically simulated [2,14].

Resistively detected NMR, performed in the proximity of the ring structure, reveals no signal on its two sides, like positions B, B', C, and C' in Fig. 1. In contrast, inside the ring structure, such as position A in Fig. 1, pronounced NMR signals were observed. NMR lines for both cases are shown in Figs. 2(a)–2(c). The relative change of R_{xx} is typically about 1% at resonance at an estimated rf power about 0.1 mW at the sample. The resonant frequencies at different V_g agree well with the theoretical values, indicated by the vertical dashed lines in Fig. 2(b). Upon resonance, R_{xx} in all NMR lines shows a sharp decrease followed by a much slower relaxation process back to its original value, which is characterized by the nuclear spin-lattice relaxation time constant, T_1, as will be discussed.

To further confirm the NMR signal, NMR lines were recorded at different magnetic fields inside the ring structure, as shown in Fig. 2(d). The resonance shows the expected blueshift with increasing B. The frequencies of the minima in the NMR lines, plotted in the inset, exhibit a linear relationship with B, and are slightly above the theoretical values denoted by the dashed line. Nevertheless, Fig. 2(e) reveals that the NMR line form is strongly dependent on frequency sweeping direction and speed. The slower the frequency sweeps, the closer the minima frequency approaches the expected theoretical value.

Although the nuclear polarization can be built up thermally at very low temperatures [9], we believe the resistively detected NMR described here is due to the electron and nuclear spin dynamic polarization effect [15–17]. For the 2D electron system in GaAs, the contact hyperfine interaction between the nuclear spin $\mathbf{I}$ and the electron spin $\mathbf{S}$ can be expressed as $\mathbf{AI} \cdot \mathbf{S} = \frac{A}{2}(I^+S^- + I^-S^+) + AI_zS_z$, where A is the hyperfine coupling constant [18]. Because of the term $\frac{A}{2}(I^+S^- + I^-S^+)$, a nuclear spin flops,

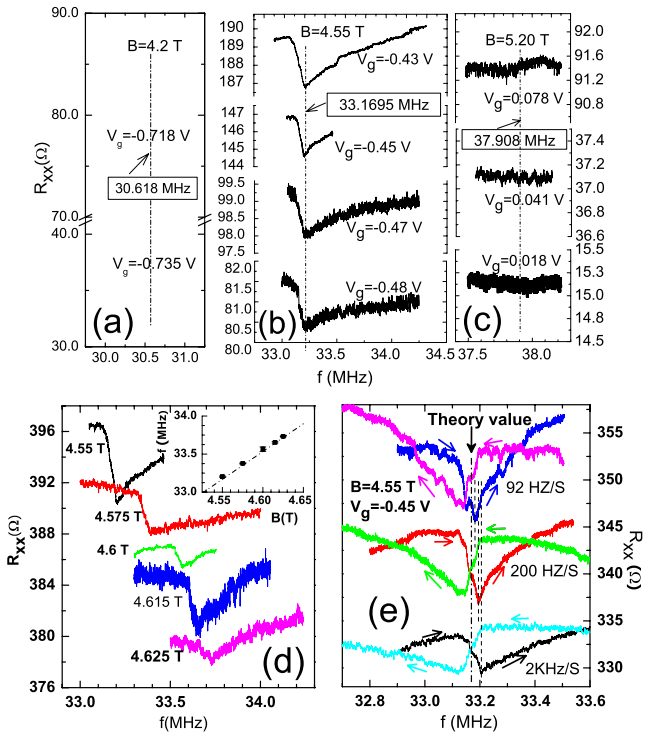

FIG. 2 (color online). (a),(b), and (c) show NMR signals close to positions C, A, and B dotted in Fig. 1, respectively. (d) NMR resonances at different magnetic fields inside the ring structure. Inset shows the resonance frequency as a function of magnetic field. (e) NMR signals at three frequency scanning speeds, and in opposite sweeping direction. In above figures, theoretical NMR values, assuming $\gamma = 7.29$ MHz/T for ^{75}As, are drawn by the dot-dashed lines.

$\downarrow\Rightarrow\uparrow$, when an electron spin flips, $\uparrow\Rightarrow\downarrow$. Nuclear spins that have once flopped hardly relax back because of their longer relaxation time, T_1, which is on the order of minutes, relative to that of the electrons. Hence up-spin nuclei pile up to develop a strong nuclear polarization I_z, which is parallel to the external magnetic field B. It will reduce the effective electron spin-flip energy,

$$E_z = g^*\mu_B B S_z + A\langle I_z\rangle S_z, \tag{1}$$

as $g^* < 0$ [9]. When the NMR resonance condition is matched, the nuclear spins are depolarized and the electron Zeeman energy increases consequently. Since R_{xx} is dependent on the energy gap of the energy spectrum, ΔE, and thermally activated according to $R_{xx} \propto \exp(-\Delta E/2kT)$, the NMR is manifested by a drop in R_{xx}, as shown by all the NMR lines in Fig. 2.

The observed prominent (absent) NMR signal inside (outside) the ring structure in Figs. 2(a)–2(c), is well correlated with the spin polarization of the picture depicted in Fig. 5 of Ref. [1]. Inside the ring along the $\nu = 6$ line, the topmost two occupied LLs from different subbands have the same spin orientation and hence $S_z = 1$ in

Eq. (1). Accordingly, the NMR signal was observed in Fig. 2(b). Whereas outside the ring along the $\nu = 6$ line, it is a normal paramagnetic state where spin split LLs of the same subband are completely filled. Hence $S_z = 0$ in Eq. (1), and NMR cannot be expected. Nevertheless, it is noteworthy that a spin polarized state alone is not sufficient to give rise to NMR in this two-subband system. For instance, NMR detection, which was performed around $\nu = 5$ did not reveal any noticeable signal.

To gain more insight into the nature of the state inside the ring, we studied the coupling between the nuclei and electrons by measuring the nuclear spin-lattice relaxation time, T_1, at various positions inside the ring structure. Figure 3(a) shows the procedure for determining T_1. At I, rf was tuned into resonance, and R_{xx} decays exponentially into a steady state due to the saturation of the nuclear depolarization. Then at II, with the frequency switching back to off resonance, nuclei gradually restore their polarization owing to the interaction with the electron spin bath. Consequently, R_{xx} slowly relaxes back to its original value, following an exponential function of the form $R_{xx} = \alpha + \beta e^{(-t/T_1')}$. T_1' is the time constant, which is approximately equal to the nuclear spin-lattice relaxation time T_1, if $g\mu_B B_N \ll 2k_B T$ and the rf power is small [10].

The obtained values of T_1 are plotted in Fig. 3(b) as a function of B for different locations inside the ring structure, marked by dots in the inset picture. These positions, with their successively diminishing resistance, represent a path progressively leading to the center of the ring structure. T_1 rapidly drops from 450 to 95 s toward the ring center, as electrons become more localized. This correlation of T_1 with localization is *opposite* to the usual relation in the quantum Hall regime, $T_1^{-1} \propto D(E) \propto \rho_{xx}$, where $D(E)$ is the density of states [9,19]. While we do not exactly know the mechanism for this enhanced nuclear spin relaxation, a recent work suggested that, for a ferromagnetic state, the relaxation is expected to be limited by spin-textured quasiparticles induced by disorder [15]. However, one needs to know how the disorder varies in the $n - B$ plane within the ring in order to compare with the data in Fig. 3(b).

NMR measurements were performed at elevated temperatures, as shown in Fig. 4. The relative change of

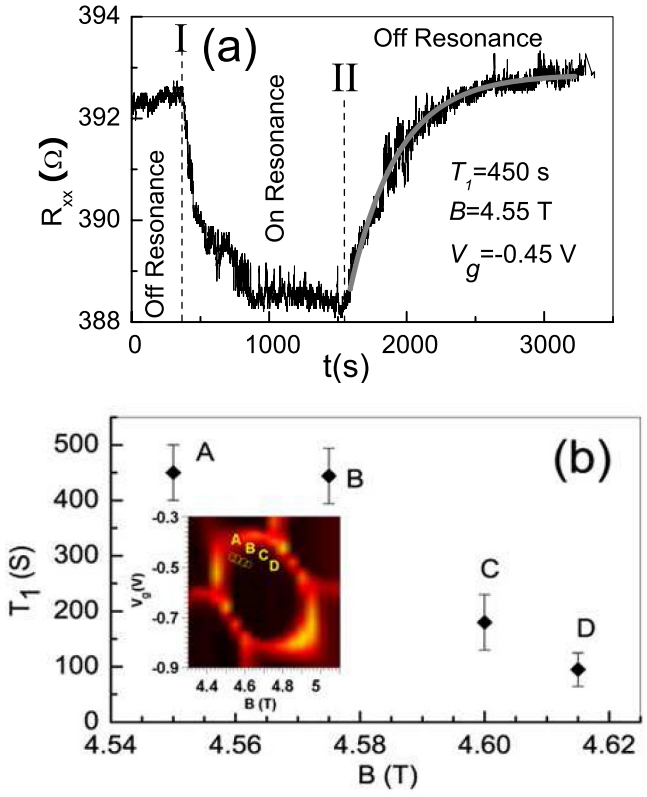

FIG. 3 (color online). (a) the principle of measuring T_1 by recording time evolution of R_{xx} irradiated by rf, initially off resonance, on resonance at 33.1695 MHz (position I), and finally off resonance (position II). T_1 is determined by an exponential fit to the experimental data shown by the thick gray curve. (b) T_1, measured at dots A(4.55 T, −0.45 V), B(4.575 T, −0.459 V), C(4.6 T, −0.468 V), and D(4.615 T, −0.475 V) in the inset graph, exhibits a declining tendency towards the ring center.

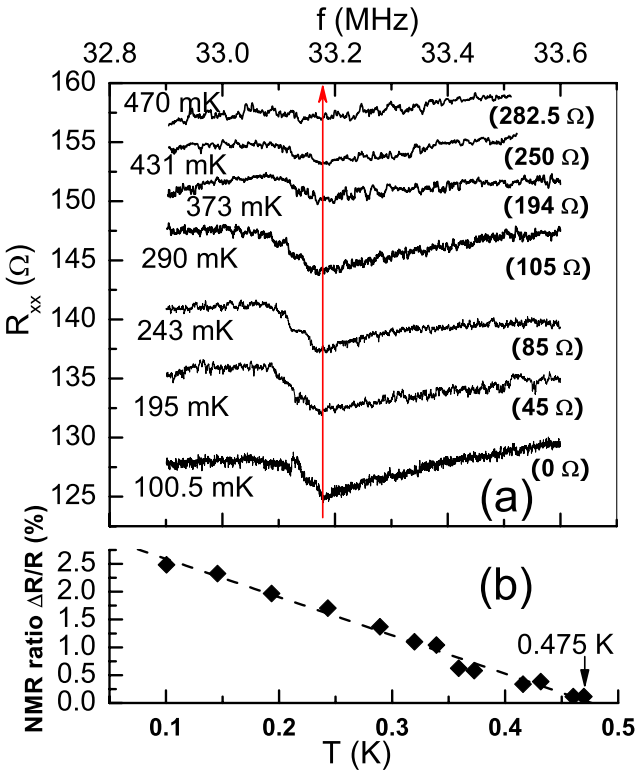

FIG. 4 (color online). (a) variable temperature measurement of NMR lines at $B = 4.55$ T and $V_g = -0.45$ V. The number in brackets is the amount of negative shift along y axis for each trace. The vertical line with arrowhead shows the gradual vanishing of the NMR signal when temperature rises. (b) The NMR ratio $\Delta R/R$ versus temperature. The dashed line is a linear fit with an extrapolation to x axis at 475 mK.

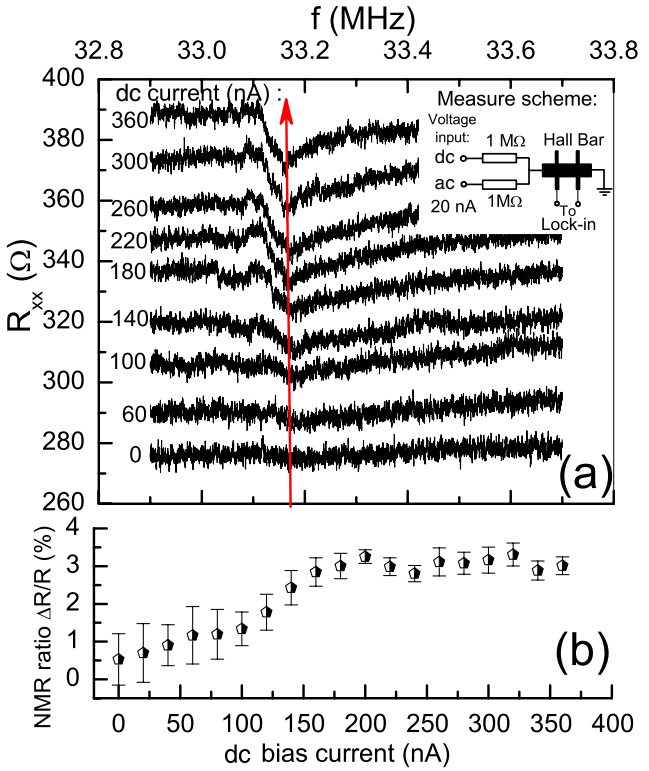

FIG. 5 (color online). (a) The enhancement of the NMR signal by the dc biasing current, indicated by the vertical line with arrowhead, at $B = 4.55$ T, $V_g = -0.40$ V, and $T = 85$ mK. The inset shows the measuring principle. Each curve was negatively shifted along y axis by 0, 0, 40, 80, 115, 150, 180, 200, and 230 Ω, from bottom to top. (b) The NMR ratio $\Delta R/R$ versus biasing current.

resistance at NMR resonance decays almost linearly with the temperature, and vanishes completely at 475 mK. T_1 as a function of temperature has also been quantitatively measured up to 250 mK, and does not reveal any noticeable temperature dependence. The measurement of T_1 above 250 mK is hindered by the weak NMR signal as the uncertainty in T_1 becomes unacceptably large. The fact that T_1 is almost temperature independent is consistent with the observation in the ferromagnetic phase of a bilayer system [15].

To investigate the mechanism of the polarized nuclear spins, current dependence of the NMR signal was studied, and is depicted in Fig. 5(a). In this measurement, the sample resistance was measured with a low ac current of 20 nA, while ramping the dc current in a wide range to bias the sample. Figure 5(b) indicates that the NMR signal is enhanced by a factor of 6 in the low current range up to 200 nA, and then saturates. This is opposite to the elevated temperature effect shown in Fig. 4. The data thus demonstrate experimentally that the observed nuclear spin polarization cannot be built thermally and must be gained by some dynamic mechanism. It is a well-known fact that the electrical current can efficiently induce electron spin-flip and nuclear spin-flop processes near the ferromagnetic phase of the $\nu = 2/3$ fractional quantum Hall state [15–17]. Since a ferromagnetic state can spontaneously separate into domains, as the applied current forces electrons to scatter between adjacent domains with different spin but almost degenerate energy, the nuclei in the neighborhood can become polarized. Adapting this picture of dynamic polarization, we can imagine that strong nuclear polarization observed at high temperatures under a biasing current in our experiment are consistent with the fact that the ring state consists of spontaneously polarized electron spins.

In conclusion, resistively detected NMR was detected only inside the ringlike structure in the phase diagram of a two-subband electron system. The associated nuclear spin-lattice relaxation time decays rapidly towards the center of the ring. The NMR signal persists to temperatures as high as 470 mK, and shows a clear dynamic pumping effect by the biasing current. These findings are consistent with the notion that there is a ferromagnetic state inside the ring structure facilitated by preferential alignment of electron spins from different subband in an external magnetic field.

The authors would like to thank W. G. Clark for helpful discussions, and B. Alavi for technical assistance. This work is supported by the NSF under Grant No. DMR-0404445.

[1] X. C. Zhang D. R. Faulhaber, and H. W. Jiang, Phys. Rev. Lett. **95**, 216801 (2005).
[2] C. Ellenberger *et al.*, Phys. Rev. B **74**, 195313 (2006).
[3] K. Muraki, T. Saku, and Y. Hirayama, Phys. Rev. Lett. **87**, 196801 (2001).
[4] X. C. Zhang, I. Martin, and H. W. Jiang, Phys. Rev. B **74**, 073301 (2006).
[5] G. F. Giuliani and J. J. Quinn, Phys. Rev. B **31**, 6228 (1985); Surf. Sci. **170**, 316 (1986).
[6] A. J. Daneshvar *et al.*, Phys. Rev. Lett. **79**, 4449 (1997).
[7] J. H. Smet *et al.*, Nature (London) **415**, 281 (2002).
[8] O. Stern *et al.*, Phys. Rev. B **70**, 075318 (2004).
[9] W. Desrat *et al.*, Phys. Rev. Lett. **88**, 256807 (2002).
[10] G. Gervais *et al.*, Phys. Rev. Lett. **94**, 196803 (2005).
[11] I. B. Spielman *et al.*, Phys. Rev. Lett. **94**, 076803 (2005).
[12] S. E. Barrett *et al.*, Phys. Rev. Lett. **74**, 5112 (1995); R. Tycko, S. E. Barret *et al.*, Science **268**, 1460 (1995).
[13] The wafer was purchased from IQE Inc., http://www.iqep.com.
[14] G. J. Ferreira, H. J. P. Freire, and J. C. Egues, Phys. Status Solidi C **3**, 4364 (2006).
[15] N. Kumada, K. Muraki, and Y. Hirayama, Science **313**, 329 (2006).
[16] S. Kronmüller *et al.*, Phys. Rev. Lett. **81**, 2526 (1998).
[17] S. Kraus *et al.*, Phys. Rev. Lett. **89**, 266801 (2002).
[18] M. Dobers *et al.*, Phys. Rev. Lett. **61**, 1650 (1988).
[19] I. D. Vagner and T. Maniv, Phys. Rev. Lett. **61**, 1400 (1988); A. Berg *et al.*, Phys. Rev. Lett. **64**, 2563 (1990).